International Journal of Applied Pharmaceutics

ISSN- 0975-7058 Vol 16, Issue 5, 2024

Original Article

THE BINARY AND TERNARY AMORPHOUS SYSTEMS OF CANDESARTAN CILEXETIL PREPARATION TO IMPROVE ITS SOLUBILITY

FIKRI ALATAS*, HESTIARY RATIH, TITTA HARTYANA SUTARNA, MUHAMAD LUTHFI FAUZI

Pharmaceutics Group, Faculty of Pharmacy, Universitas Jenderal Achmad Yani, Jl. Terusan Jenderal Sudiman, Cimahi, West Java-40521, Indonesia

***Corresponding author: Fikri Alatas; *Email: fikri.alatas@lecture.unjani.ac.id**

Received: 15 Apr 2024, Revised and Accepted: 02 Jul 2024

ABSTRACT

Objective: The objectives of this work was to prepare the binary and ternary amorphous systems of Candesartan cilextil (CAN), characterize these, and evaluate their influence on solubility.

Methods: CAN was prepared in three amorphous systems, namely Candesartan cilexetil-l-Arginine (CAN-ARG) binary Co-Amorphous System (CAMS), CAN with 10, 20, and 30% of Polyvinylpyrrolidone K25 (CAN-PVP K25) Amorphous Solid Dispersion (ASD), and CAN-ARG with 10, 20, and 30% of PVP K25 (CAN-ARG-PVP K25) ternary CAMS. All amorphous systems were characterized by polarizing microscopy and differential scanning calorimetry (DSC) methods, while the degree of crystallinity was calculated based on powder X-ray diffraction (PXRD) patterns. The solubility test of all amorphous systems of CAN was carried out respectively in water solvent (25±0.5 °C) and phosphate buffer solution with a pH of 6.5 that contained 0.70% polysorbate 20 at 37±0.5 °C.

Results: Polarization microscope images showed no birefringence in CAN-ARG and CAN-ARG-PVP K25 CAMS, but strong birefringence in CAN-PVP K25. DSC thermograms show the glass transition of CAN-ARG-PVP-K25 was in the range 101-120.8 °C higher than CAN-PVP-K25 (84.1-87.5 °C) and CAN-ARG (53.5 °C). The crystallinity degrees of CAN, CAN-ARG, CAN-PVP K25, and CAN-ARG-PVPK25 calculated based on powder X-ray diffractogram data were 73.68, 7.52, 17.20, and 0.02%, respectively. The order of solubility of CAN in water and phosphate buffer solution with a pH of 6.5 that contains 0.70% polysorbate 20 was CAN-ARG-PVP-K25>CAN-ARG>CAN-PVP-K25>CAN.

Conclusion: The synthesis of binary and ternary amorphous CAN has resulted in positive outcomes, enhancing its solubility.

Keywords: Candesartan cilexetil, l-Arginine, Polyvinylpyrrolidone K25, Amorphous, Solubility

DOI: https://dx.doi.org/10.22159/ijap.2024v16i5.51141 Journal homepage: https://innovareacademics.in/journals/index.php/ijap

INTRODUCTION

The limited solubility in water of an Active Pharmaceutical Ingredient (API) is known to be one of the significant problems in solid dosage form formulation [1]. The topic of low solubility in water is a significant concern in the advance of drug formulations, as it leads to limited dissolution, inadequate bioavailability, and consequently unsatisfactory therapeutic effectiveness [2]. Amorphization of crystalline materials using various techniques has been intensively researched as a means of overcoming the problem of a growing number of APIs being insufficiently water-soluble, including Amorphous Solid Dispersion (ASD) [3–8].

ASD manufacturing has attracted significant attention in academic and industrial circles as an additional technique. Solid dispersions can be explained as molecular combinations of APIs with low solubility in water, distributed in a hydrophilic polymer [9]. The purpose of solid dispersion is to increase the surface area, as well as increase the solubility and stability of APIs [10, 11]. ASD refers to a formulation in which API is dispersed in a vehicle that exhibits an amorphous form. This concept suggests that the conversion of crystalline APIs to their amorphous form is achieved through their blending with amorphous polymers [12]. Although this technique offers clear benefits, it also has several disadvantages, such as the difficulty in producing and processing solid dispersions due to the hygroscopic nature of the carrier polymer and the need for large amounts of polymer to increase the solubility [6, 13, 14].

Currently, the use of Co-Amorphous Systems (CAMS) has developed progressively recognized in the last decade as a solution to the shortcomings of solid dispersion techniques. CAMS is defined as combining APIs with small molecules as opposed to using macromolecules for example, polymers that create a homogenous single-phase [15, 16]. The term CAMS generally refers to binary CAMS between an API and a small molecule, such as amino acids, organic acids, and other APIs [17, 18]. Molecular interactions between the components in these systems are important. Nevertheless, under some conditions, the efficacy of solubilization by binary CAMS is inadequate, therefore necessitating the inclusion of a third excipient, such as a surfactant, polymer, or another small molecule to improve solubility [19-21]. The addition of a third material in the binary CAMS is known as ternary CAMS to differentiate it from ternary ASD [17].

Candesartan cilexetil (CAN), a prodrug of candesartan is a commonly employed antihypertensive agent that functions by inhibiting the angiotensin II receptor. From a pharmacokinetic perspective, it was observed that the prodrug has a rather low oral bioavailability [22]. CAN has been grouped as a class II drug in the biopharmaceutics classification system (BCS) due to its solubility in pH values relevant to physiological processes and its absorption characteristics [23].

In previous research, we have succeeded in manufacturing binary CAMS from CAN with l-Arginine (ARG) using the liquid-assisted grinding method and increasing its solubility in water [24]. However, based on the Powder X-Ray Diffraction (PXRD) pattern in that study, quite high-intensity peaks were still visible, indicating that there were still crystalline areas in the Candesartan-cilexetil-l-Arginine (CAN-ARG) binary CAMS. In this study, we added Polyvinylpyrrolidone (PVP) K25 polymer to CAN-ARG binary CAMS to create CAN-ARG-PVP K25 ternary CAMS. PVP is a polymer that can be used as a third material in preparation of binary ASD [25] or ternary CAMS [1, 26–29]. In addition, this study also involved the preparation of a binary ASD consisting of CAN and PVP K25 (referred to as CAN-PVP K25). The objective of the study was to prepare the binary and ternary amorphous systems of CAN, characterize these, and evaluate their influence on solubility.

MATERIALS AND METHODS

Materials

The utilized chemicals consist of CAN sourced from Afine Chemical Limited, China, l-arginine obtained from Merck in

Indonesia, and PVP K25 supplied by BASF in Indonesia. Ethanol, phosphate buffer, and polysorbate 80 were procured from Merck Indonesia.

The CAN-ARG binary CAMS preparation

The liquid-assisted grinding method was used to prepare the CAN-ARG binary CAMS [24, 30]. A binary CAMS was generated by grinding a mixture of 2.202 g (5 mmol) of CAN, 0.871 g (5 mmol) of ARG, and eight drops of ethanol in a Retsch RM 200 mortar grinder for ten minutes. The CAN-ARG binary CAMS soft mass was placed in a desiccator and subsequently subjected to a drying process. The CAN-ARG binary CAMS was pulverized and subsequently sieved to ensure particle size uniformity, with the particles passing through a 60-mesh sieve.

The CAN-PVP K25 binary ASD preparation

The CAN-PVP K25 binary ASD was synthesized using the solvent evaporation technique [31]. A quantity of 2.202 g of CAN was combined with a certain quantity of PVP K25 that corresponded to CAN concentrations of 10%, 20%, and 30% in three separate evaporating dishes. A volume of two ml of ethanol was introduced into each evaporating dish and agitated until complete dissolution of CAN and PVP K25 occurred. The solution was allowed to stand for one day, during which the ethanol underwent evaporation, resulting in the formation of the CAN-PVP K25 binary ASD. The CAN-PVP K25 binary ASD was pulverized and subsequently passed through a 60-mesh sieve.

The CAN-ARG-PVP K25 ternary CAMS preparation

The CAN-ARG-PVP K25 ternary CAMS was produced by the solvent evaporation technique [32, 33]. Three quantities of 3.0 g of CAN-ARG binary CAMS were individually placed into three evaporating dishes and combined with specific quantities of PVP K25 that corresponded to 10, 20, and 30% of the mass of CAN. The dissolution process involved the addition of two milliliters of ethanol to each combination. The solution was allowed to stand for one day, during which time the ethanol underwent evaporation, resulting in the formation of a solid material known as CAN-ARG-PVP K25 ternary CAMS. The CAN-ARG-PVP K25 ternary CAMS samples were processed by pulverization and separation via a 60-mesh sieve.

Characterization by polarizing microscope

In this study, we analyzed various samples, including CAN, ARG, PVP K25, CAN-ARG binary CAMS, and CAN-PVP K25 (at concentrations of 10, 20, and 30%) binary ASD, as well as CAN-ARG-PVP K25 (at concentrations of 10, 20, and 30%) ternary CAMS. Each sample consisted of 1-3 mg. The utilization of a polarizing microscope equipped with a digital camera allowed for the observation of crystal morphology and the identification of birefringence.

Thermal analysis by Differential Scanning Calorimeter (DSC)

The thermal analysis of DSC was carried out on CAN, ARG, PVP K25, CAN-ARG, CAN-PVP K25 (10, 20, and 30%) binary ASD, and CAN-ARG-PVP K25 (10, 20, and 30%) ternary CAMS. The powder samples were precisely measured and placed in aluminum crucible pans. The pans were then sealed with airtight covers. The aluminum crucible pan was placed within the Shimadzu DSC-6 Plus and exposed to a temperature scan ranging from 30 to 250 °C, with an average heating rate of 10° per minute.

Characterization and determination of degree of crystallinity by PXRD method

A thin aluminum sample container has been filled with approximately 500 mg each of CAN powder, ARG, PVP K25, CAN-ARG binary CAMS, CAN-PVP K25 binary ASD, and CAN-ARG-PVP K25 ternary CAMS. The PXRD patterns were collected on a panalytical Empyrean powder X-ray diffractometer. The patterns were scanned at a scan speed of 10°/minute over a range of 5-45° 2θ angle. The 40 kV and 30 mA were set for both voltage and current. Equation 1 is used to compute the degree of crystallinity by dividing the area of crystalline peaks of diffraction (Ac) by the total of the area of crystalline peaks of diffraction (Ac) and the area of amorphous of diffraction (Aa) [34, 35].

$$\text{Degree of crystallinity} = \frac{\text{Ac}}{\text{Ac+Aa}} \text{x} 100\% \text{. ..... eq. 1}$$

Solubility test

The shaker method was used to conduct the solubility tests in water at room temperature and in the phosphate buffer solution with a pH of 6.5 that contained 0.70% polysorbate 20 at 37±0.5 °C [36]. Each vial included 50 mg of the following powders: CAN, CAN-ARG binary CAMS, CAN-PVP K25 30% binary ASD, and CAN-ARG-PVP K25 30% ternary CAMS. The vial contained five milliliters of medium. The vials were placed in an orbital shaker at room temperature, while other vials were placed in a water bath shaker at 37±0.5 °C. The vials were shaken for two days and filtered when the shaking had finished. An ultraviolet spectrophotometer was used to measure the absorbance of the filtrate at a wavelength of 251 nm.

RESULTS AND DISCUSSION

Preparation of binary and ternary amorphous CAN

Similar to previous studies, CAN-ARG binary CAMS were prepared by solvent-drop grinding method [24]. While CAN-PVP K25 binary ASD and CAN-ARG-PVP K25 ternary CAMS were prepared by solvent evaporation method. Ethanol was used as a solvent in the manufacture of the amorphous CAN because the three components involved (CAN, ARG, and PVP K25) are soluble in this solvent. Unlike CAN-ARG binary CAMS, CAN-PVP K25 binary ASD and CAN-ARG-PVP K25 ternary CAMS require more ethanol to dissolve PVP K25, so the dissolving method or solvent evaporation was used for the preparation of both these amorphous solids. Only a small amount of PVP K25 was required to prepare both CAN-PVP K25 binary ASD and CAN-ARG-PVP K25 ternary CAMS, which is only 10-30% of CAN. The aim is to prevent aggregation and hydrogel formation from the polymer, which can result in a decrease in the drug dissolution rate [37]. In addition, the utilization of a low concentration of PVP K25 serves the purpose of mitigating the potential issue of excessive unit dose size and the occurrence of recrystallization during storage, which can be attributed to the hygroscopic properties inherent in the polymer [38].

Polarizing microscope

One method that can be used to observe the formation of new crystal structures and amorphous solids is to observe the crystal shape directly with a polarizing microscope [39, 40]. The polarizing microscope images of binary and ternary amorphous CAN and its starting materials are shown in fig. 1. Polarizing microscope images of the starting materials CAN) and ARG showed strong birefringence. Strong birefringence was observed in the starting materials CAN and ARG. CAN suggests a rod-shaped crystal, whereas ARG denotes a spherulite-like crystal. On the other hand, the starting material PVP K25 did not show any birefringence, which indicates that this material was in an amorphous state. Since the CAN-ARG binary CAMS exhibits no discernible birefringence, it may be concluded that an amorphous solid was created because of the interaction between CAN and ARG. In contrast to CAN-ARG binary CAMS, CAN-PVP K25 binary ASD with all concentrations still shows birefringence from the crystal habit of CAN. This demonstrates that not all the CAN crystals can transform to amorphous due to the creation of a solid dispersion between CAN and PVP K25 of variations of 10–30% of the weight of CAN. In line with the CAN-ARG binary CAMS, the polarizing microscope images of CAN-ARG-PVP K25 ternary CAMS did not demonstrate any birefringence attributable to the crystal morphology of CAN. This observation indicates that the CAN-ARG ternary CAMS distributed within the PVP K25 polymer matrix retains its amorphous nature [41].

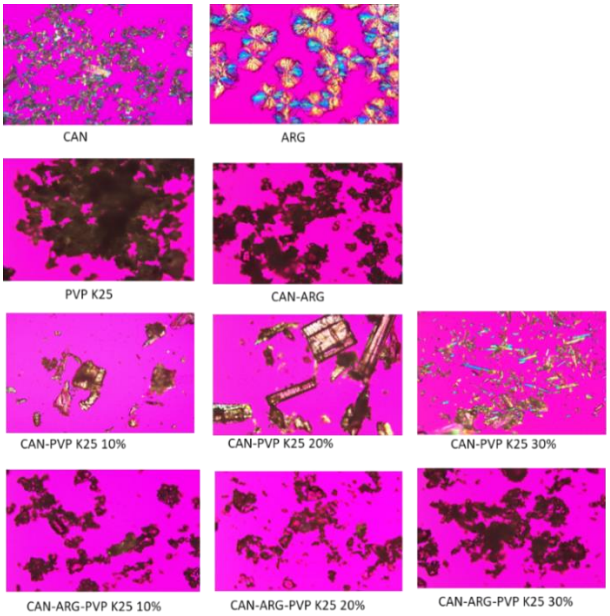

Fig. 1: Polarizing microscope images of candesartan cilexetil (CAN), l-Arginine (ARG), Polyvinylpyrrolidone K25 (PVP K25), Candesartan-cilexetil-l-Arginin (CAN-ARG) binary CAMS, Candesartan cilexetil-Polyvinylpyrrolidone K25 (CAN-PVP K25) binary ASD, and Candesartan cilexetil-l-Arginine-Polyvinylpyrrolidone K25 (CAN-ARG-PVP K25) ternary CAMS

DSC thermograms CAN-ARG binary CAMS, CAN-PVP K25 (10, 20, and 30%) binary ASD, CAN-ARG-PVP K25 (10, 20, and 30%) ternary CAMS, and their starting materials (CAN, ARG, and PVP K25) were shown in fig. 2. The DSC thermogram of the CAN starting material shows a sharp endothermic transition at 177.3 °C which was related to its melting and was followed by decomposition [42]. In contrast to the starting materials CAN and ARG, it was observed that PVP K25 did not exhibit a distinct, sharp endothermic transition. However, a noticeable glass transition was observed at a temperature of 144.7 °C. The endothermic transition exhibits an expansion within the range of around 30-80 °C, which can be attributed to the process of surface water evaporation [43]. The findings of this study suggest that the starting materials CAN and ARG exhibit a crystalline structure, whereas PVP K25 demonstrates an amorphous nature. The DSC thermogram of the CAN-ARG binary CAMS showed a glass transition at 53.5 °C. This finding demonstrates the presence of a molecular interaction between drug and coformer through hydrogen bond or co-amorphous salt, which can increase the stability of the amorphous drug [44]. The DSC thermogram of the binary ASD consisting of CAN and PVP K25 at various concentrations (10%, 20%, and 30%) reveals a glass transition occurring within the temperature range of 84.1-87.5 °C. This observation suggests the successful creation of an amorphous blend between the two components. Nevertheless, the thermograms obtained from the DSC analysis of the CAN-PVP K25 binary ASD at various concentrations (10%, 20%, and 30%) exhibit a significant endothermic transition occurring at about 109 °C. Notably, the enthalpy of fusion (ΔH_f) decreases as the concentration of PVP K25 in the system increases. This observation indicates that the change of CAN into an amorphous state is not universal, as it is dependent on the concentration of PVP K25. Specifically, a higher concentration of PVP K25 leads to a greater extent of transition from the crystal form to the amorphous form of CAN. In comparison to the CAN-PVP K25 binary ASD, the DSC thermogram of the CAN-ARG-PVP K25 ternary CAMS exhibits solely the occurrence of a glass transition, without any observable endothermic transition, across all concentrations (10%, 20%, and 30%). The glass transition temperature of the CAMS ternary system, consisting of CAN-ARG-PVP K25, exhibits an upward trend as the quantity of PVP K25 is augmented. This finding demonstrates that the incorporation of PVP K25 into CAN-ARG binary CAMS has the potential to elevate the glass transition temperature. In the context of co-amorphous systems, it is commonly postulated that an elevation in the glass transition temperature (Tg) is associated with an enhancement in physical stability [15].

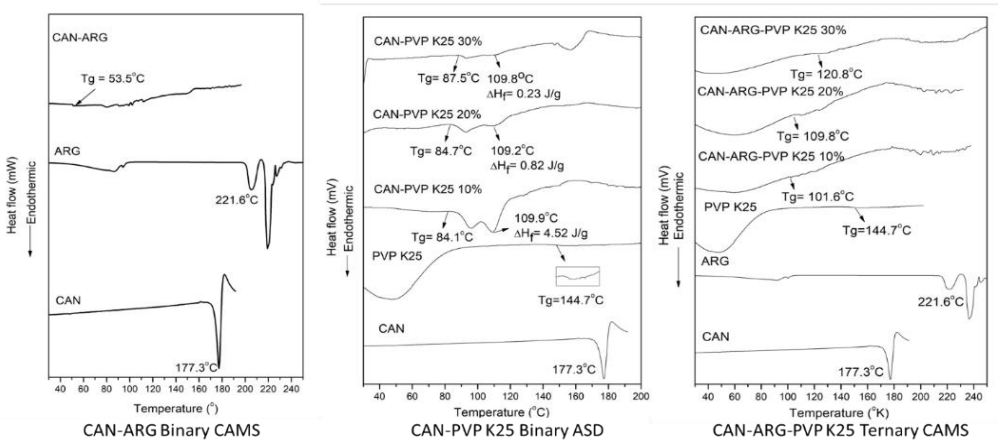

Fig. 2: Thermograms differential scanning calorimetry of Candesartan cilexetil (CAN), l-Arginine (ARG), Polyvinylpyrrolidone K25 (PVP K25), Candesartan-cilexetil-l-Arginin (CAN-ARG) binary CAMS, Candesartan cilexetil-Polyvinylpyrrolidone K25 (CAN-PVP K25) binary ASD, and Candesartan cilexetil-l-Arginine-Polyvinylpyrrolidone K25 (CAN-ARG-PVP K25) ternary CAMS

The PXRD patterns of CAN-ARG binary CAMS, CAN-PVP K25 (30%) binary ASD, CAN-ARG-PVP K25 (30%) ternary CAMS, and their starting materials are shown in fig. 3. The powder X-ray diffraction (PXRD) patterns obtained for the compounds CAN and ARG exhibited several well-defined peaks, suggesting the crystalline nature of both initial substances. The PXRD pattern of CAN is consistent with the crystalline structure of CAN form 1 as previously reported, with main peaks at 9.8, 17.2, 18.5, 19, 2, 20.2, 23.2, and 25.2 of 2θ angles [42]. In contrast to CAN and ARG, the PXRD pattern of PVP K25 demonstrated an amorphous structure. The PXRD patterns of CAN-ARG binary CAMS, CAN-PVP K25 binary ASD, and CAN-ARG-PVP K25 exhibited a reduction in the peak intensity of CAN. The successful fabrication of three amorphous systems of CAN was demonstrated by the observed transformation from a crystalline state to an amorphous state. Nevertheless, it is worth noting that in the CAN-ARG binary CAMS and CAN-PVP K25 binary ASD, there are still observable peaks corresponding to CAN, albeit with very low intensity. This suggests that the conversion of all CAN crystals into an amorphous state has not been fully achieved. The observed intensity of CAN in the CAN-PVP K25 binary ASD appears to be higher than that in the CAN-ARG binary CAMS.

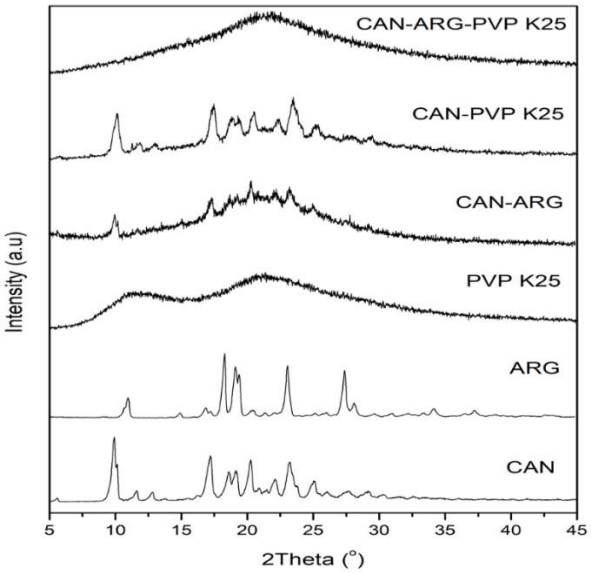

Fig. 3: Diffractograms of candesartan cilexetil (CAN), l-Arginine (ARG), Polyvinylpyrrolidone K25 (PVP K25), Candesartan-cilexetil-l-Arginin (CAN-ARG) binary CAMS, Candesartan cilexetil-Polyvinylpyrrolidone K25 (CAN-PVP K25) binary ASD, and Candesartan cilexetil-l-Arginine-Polyvinylpyrrolidone K25 (CAN-ARG-PVP K25) ternary CAMS

Calculation of the degree of crystallinity was used to determine the success of the transformation from a crystalline to an amorphous form of CAN in various amorphous systems of CAN. According to the findings presented in table 1, the utilization of CAN-ARG-PVP K25 ternary CAMS can induce a complete transformation of the crystal structure of CAN, resulting in its conversion into an amorphous form. Conversely, the formation of CAN-ARG binary CAMS and CAN-PVP K25 binary ASD did not bring about such a change, as CAN remains in a crystalline form. The crystallinity of the CAN-PVP K25 binary ASD was 2.3 times greater than that of the CAN-ARG binary CAMS. The significant level of crystallinity observed in the CAN-PVP K25 binary ASD can be attributed to the presence of PVP K25, which constitutes up to 30% of the total weight of CAN. This substantial amount of PVP K25 prevents the complete conversion of CAN into an amorphous form. The CAN-ARG-PVP K25 ternary CAMS exhibited a significantly low degree of crystallinity, suggesting a complete transformation of CAN into an amorphous state.

Table 1: Degree of crystallinity of binary and ternary amorphous of CAN

Materials	Degree of crystallinity (%)
CAN	73.68
CAN-ARG	7.51
CAN-PVP K25 (30%)	17.20
CAN-ARG-PVP K25 (30%)	0.02

CAN: Candesartan cilexetil, CAN-ARG: Candesartan-cilexetil-l-Arginin, CAN-PVP K25: Candesartan cilexetil-Polyvinylpyrrolidone K25, CAN-ARG-PVP K25: Candesartan cilexetil-l-Arginine-Polyvinylpyrrolidone K25

Solubility

The results of the solubility test are presented in table 2. The solubility of CAN is greater in phosphate buffer solution with a pH of 6.5, which contains 0.70% polysorbate 20, at a temperature of 37±0.5 °C, compared to its solubility in water at ambient temperature. The solubility test results demonstrated an augmentation in the solubility of CAN in both test media after the formation of binary and ternary CAMS. The solubility of CAN-ARG binary CAMS, CAN-PVP K25 binary ASD, and CAN-ARG-PVP K25 (30%) ternary CAMS in water is significantly higher compared to CAN, with solubility values of 315, 39, and 428 times that of CAN, respectively. Similarly, in phosphate buffer solution 0.05M at pH 6.5 containing 0.70% polysorbate 20, the solubility of these compounds is also significantly higher, with solubility values of 14, 5, and 16 times that of CAN, respectively. The CAN-ARG-PVP K25 (30%) ternary CAMS has a higher solubility than the two binaries amorphous of CAN. The limited enhancement in the solubility of CAN in the CAN-PVP K25 binary ASD can be attributed to its relatively higher degree of crystallinity in comparison to binary and ternary CAMS. The disparity in the notable enhancement of CAN solubility between CAN-PVP K25 binary ASD and binary and ternary CAMS is presumably attributable to the incorporation of ARG in both CAMS. The ionization of CAN, a weak acid, is induced by the presence of ARG, a weak base [45].

Table 2: Solubility of binary and ternary amorphous of CAN compared with pure CAN

Materials	Solubility (mg/ml)	
	Water (room temperature)	pH 6.5 (37±0.5 °C)
CAN	0.009± 0.001[a]	0.289±0.008
CAN-ARG	2.837±0.114[a]	3.940±0,018
CAN-PVP K25 (30%)	0.353±0.126	1.459±0.077
CAN-ARG-PVP K25 (30%)	3.854±0.023	4.496±0.027

Results presented as mean±SD, n= 3, [a]= The data was adopted from a previous study [24], CAN: Candesartan cilexetil, CAN-ARG: Candesartan-cilexetil-l-Arginin, CAN-PVP K25: Candesartan cilexetil-Polyvinylpyrrolidone K25, CAN-ARG-PVP K25: Candesartan cilexetil-l-Arginine-Polyvinylpyrrolidone K25

CONCLUSION

The effective preparation and characterization of binary and ternary amorphous forms of CAN have been achieved. The characterization by polarizing microscope, DSC, and PXRD methods indicates that not all CAN in CAN-ARG binary CAMS and CAN-PVP K25 binary ASD transform into the amorphous state. However, in the case of CAN-ARG-PVP K25 ternary CAMS, it was observed that all the CAN have indeed transformed into an amorphous form. These binary and ternary amorphous systems enhanced the solubility of CAN in water and a pH 6.5 buffer solution. The CAN-ARG-PVP K25 ternary CAMS exhibits higher solubility than the CAN-ARG binary CAMS and CAN-PVP K25 binary ASD.

ACKNOWLEDGMENT

The authors thank the Institute for Research and Community Service at Universitas Jenderal Achmad Yani for providing financial support for this study.

AUTHORS CONTRIBUTIONS

FA: designed the research, analyzed and interpreted the results of microscope polarization, DSC, PXRD, and calculated crystallinity tests, and wrote the article. HR: carried out solubility tests and analyzed them, THS: prepared binary co-amorphous systems, MLF: prepared binary amorphous solid dispersion and ternary co-amorphous systems.

CONFLICT OF INTERESTS

The authors have disclosed that they have no conflicts of interest.

REFERENCES

1. Riekes MK, Engelen A, Appeltans B, Rombaut P, Stulzer HK, Van Den Mooter G. New perspectives for fixed-dose combinations of poorly water-soluble compounds: a case study with ezetimibe and lovastatin. Pharm Res. 2016;33(5):1259-75. doi: 10.1007/s11095-016-1870-z, PMID 26857899.
2. Shi Q, Moinuddin SM, Cai T. Advances in coamorphous drug delivery systems. Acta Pharm Sin B. 2019;9(1):19-35. doi: 10.1016/j.apsb.2018.08.002, PMID 30766775.
3. Laitinen R, Lobmann K, Strachan CJ, Grohganz H, Rades T. Emerging trends in the stabilization of amorphous drugs. Int J Pharm. 2013;453(1):65-79. doi: 10.1016/j.ijpharm.2012.04.066, PMID 22569230.
4. Kanaujia P, Poovizhi P, Ng WK, Tan RB. Amorphous formulations for dissolution and bioavailability enhancement of poorly soluble APIs. Powder Technol. 2015;285:2-15. doi: 10.1016/j.powtec.2015.05.012.
5. Maleki A, Kettiger H, Schoubben A, Rosenholm JM, Ambrogi V, Hamidi M. Mesoporous silica materials: from physico-chemical properties to enhanced dissolution of poorly water-soluble drugs. J Control Release. 2017;262:329-47. doi: 10.1016/j.jconrel.2017.07.047, PMID 28778479.
6. Tekade AR, Yadav JN. A review on solid dispersion and carriers used therein for solubility enhancement of poorly water-soluble drugs. Adv Pharm Bull. 2020;10(3):359-69. doi: 10.34172/apb.2020.044, PMID 32665894.
7. Mishra DK, Dhote V, Bhargava A, Jain DK, Mishra PK. Amorphous solid dispersion technique for improved drug delivery: basics to clinical applications. Drug Deliv Transl Res. 2015;5(6):552-65. doi: 10.1007/s13346-015-0256-9, PMID 26306524.
8. Kim DH, Kim YW, Tin YY, Soe MT, Ko BH, Park SJ. Recent technologies for amorphization of poorly water-soluble drugs. Pharmaceutics. 2021;13(8):1318. doi: 10.3390/pharmaceutics13081318, PMID 34452279.
9. Chiou WL, Riegelman S. Pharmaceutical applications of solid dispersion systems. J Pharm Sci. 1971;60(9):1281-302. doi: 10.1002/JPS.2600600902, PMID 4935981.
10. Haser A, Zhang F. New strategies for improving the development and performance of amorphous solid dispersions. AAPS PharmSciTech. 2018;19(3):978-90. doi: 10.1208/s12249-018-0953-z, PMID 29340977.
11. Ji Y, Paus R, Prudic A, Lubbert C, Sadowski G. A novel approach for analyzing the dissolution mechanism of solid dispersions. Pharm Res. 2015;32(8):2559-78. doi: 10.1007/s11095-015-1644-z, PMID 25715696.
12. Srivastava A, Khan MA, Bedi S, Bhandari U. Design, optimization, and characterization of a novel amorphous solid dispersion formulation for enhancement of solubility and dissolution of ticagrelor. Int J App Pharm. 2023;15(4):296-305. doi: 10.22159/ijap.2023v15i4.47618.
13. Tran P, Pyo YC, Kim DH, Lee SE, Kim JK, Park JS. Overview of the manufacturing methods of solid dispersion technology for improving the solubility of poorly water-soluble drugs and application to anticancer drugs. Pharmaceutics. 2019;11(3):1-26. doi: 10.3390/pharmaceutics11030132, PMID 30893899.
14. Srinarong P, De Waard H, Frijlink HW, Hinrichs WL. Improved dissolution behavior of lipophilic drugs by solid dispersions: the production process as starting point for formulation considerations. Expert Opin Drug Deliv. 2011;8(9):1121-40. doi: 10.1517/17425247.2011.598147, PMID 21722000.
15. Dengale SJ, Grohganz H, Rades T, Lobmann K. Recent advances in co-amorphous drug formulations. Adv Drug Deliv Rev. 2016;100:116-25. doi: 10.1016/j.addr.2015.12.009, PMID 26805787.
16. Liu J, Grohganz H, Lobmann K, Rades T, Hempel NJ. Co-amorphous drug formulations in numbers: recent advances in co-amorphous drug formulations with focus on co-formability, molar ratio, preparation methods, physical stability, *in vitro* and *in vivo* performance, and new formulation strategies. Pharmaceutics. 2021;13(3). doi: 10.3390/pharmaceutics13030389, PMID 33804159.
17. Moinuddin SM, Ruan S, Huang Y, Gao Q, Shi Q, Cai B. Facile formation of co-amorphous atenolol and hydrochlorothiazide mixtures via cryogenic-milling: enhanced physical stability, dissolution and pharmacokinetic profile. Int J Pharm. 2017;532(1):393-400. doi: 10.1016/j.ijpharm.2017.09.020, PMID 28893583.
18. Yarlagadda DL, Sai Krishna Anand V, Nair AR, Navya Sree KS, Dengale SJ, Bhat K. Considerations for the selection of co-formers in the preparation of co-amorphous formulations. Int J Pharm. 2021;602:120649. doi: 10.1016/j.ijpharm.2021.120649.
19. Li F, Li L, Wang S, Yang Y, Li J, Liu D. Improved dissolution and oral absorption by co-grinding active drug probucol and ternary stabilizers mixtures with planetary beads-milling method. Asian J Pharm Sci. 2019;14(6):649-57. doi: 10.1016/j.ajps.2018.12.001, PMID 32104491.
20. Aljohani M, McArdle P, Erxleben A. Dual-drug amorphous formulation of gliclazide. Drug Dev Ind Pharm. 2021;47(2):302-7. doi: 10.1080/03639045.2021.1879838, PMID 33492999.
21. Fang X, Hu Y, Yang G, Shi W, Lu S, Cao Y. Improving physicochemical properties and pharmacological activities of ternary co-amorphous systems. Eur J Pharm Biopharm. 2022 Dec 1;181:22-35. doi: 10.1016/j.ejpb.2022.10.008, PMID 36283631.

22. Figueroa Campos A, Sanchez Dengra B, Merino V, Dahan A, Gonzalez Alvarez I, Garcia Arieta A. Candesartan cilexetil *in vitro–in vivo* correlation: predictive dissolution as a development tool. Pharmaceutics. 2020;12(7):633. doi: 10.3390/pharmaceutics12070633, PMID 32640620.
23. Dudhipala N, Veerabrahma K. Candesartan cilexetil loaded solid lipid nanoparticles for oral delivery: characterization, pharmacokinetic and pharmacodynamic evaluation. Drug Deliv. 2016;23(2):395-404. doi: 10.3109/10717544.2014.914986, PMID 24865287.
24. Alatas F, Mutmainah ES, Ratih H, Sutarna TH, Soewandhi SN. Identification of candesartan cilexetil-l-arginine co-amorphous formation and its solubility test. Borneo J Pharm. 2022;5(1):27-34. doi: 10.33084/bjop.v5i1.2942.
25. Kaushik R, Verma R, Budhwar V, Kaushik D. Investigation of solid dispersion approach for the improvement of pharmaceutical characteristics of telmisartan using a central composite design. Int J App Pharm. 2023;15(5):245-54. doi: 10.22159/ijap.2023v15i5.47968.
26. Pacult J, Rams Baron M, Chmiel K, Jurkiewicz K, Antosik A, Szafraniec J. How can we improve the physical stability of co-amorphous system containing flutamide and bicalutamide? The case of ternary amorphous solid dispersions. Eur J Pharm Sci. 2019;136:104947. doi: 10.1016/j.ejps.2019.06.001.
27. Ruponen M, Rusanen H, Laitinen R. Dissolution and permeability properties of co-amorphous formulations of hydrochlorothiazide. J Pharm Sci. 2020;109(7):2252-61. doi: 10.1016/j.xphs.2020.04.008, PMID 32315662.
28. Nguyen DN, Van Den Mooter G. The fate of ritonavir in the presence of Darunavir. Int J Pharm. 2014;475(1-2):214-26. doi: 10.1016/j.ijpharm.2014.08.062, PMID 25180992.
29. Liu X, Zhou L, Zhang F. Reactive melt extrusion to improve the dissolution performance and physical stability of naproxen amorphous solid dispersions. Mol Pharm. 2017;14(3):658-73. doi: 10.1021/acs.molpharmaceut.6b00960, PMID 28135108.
30. Kasten G, Lobo L, Dengale S, Grohganz H, Rades T, Lobmann K. *In vitro* and *in vivo* comparison between crystalline and co-amorphous salts of naproxen-arginine. Eur J Pharm Biopharm. 2018;132:192-9. doi: 10.1016/j.ejpb.2018.09.024, PMID 30266670.
31. Medarevic D, Cvijic S, Dobricic V, Mitric M, Djuris J, Ibric S. Assessing the potential of solid dispersions to improve dissolution rate and bioavailability of valsartan: *in vitro*-in silico approach. Eur J Pharm Sci. 2018;124:188-98. doi: 10.1016/j.ejps.2018.08.026, PMID 30144529.
32. Saberi A, Kouhjani M, Yari D, Jahani A, Asare Addo K, Kamali H. Development, recent advances, and updates in binary, ternary co-amorphous systems, and ternary solid dispersions. J Drug Deliv Sci Technol. 2023 Sep 1;86:1-26. doi: 10.1016/j.jddst.2023.104746.
33. Lu Q, Zografi G. Phase behavior of binary and ternary amorphous mixtures containing indomethacin, citric acid, and PVP. Pharm Res. 1998;15(8):1202-6. doi: 10.1023/a:1011983606606, PMID 9706050.
34. Doumeng M, Makhlouf L, Berthet F, Marsan O, Delbe K, Denape J. A comparative study of the crystallinity of polyetheretherketone by using density, DSC, XRD, and Raman spectroscopy techniques. Polym Test. 2021;93:1-10. doi: 10.1016/j.polymertesting.2020.106878.
35. Black DB, Lovering EG. Estimation of the degree of crystallinity in digoxin by X-ray and infrared methods. J Pharm Pharmacol. 1977;29(11):684-7. doi: 10.1111/j.2042-7158.1977.tb11435.x, PMID 22603.
36. Xuan ZY, Wang L Yang, Dai J kai, Liu F, Li Y Tuan, Wu Z Yong. The comparative study of cocrystal/salt in simultaneously improving solubility and permeability of acetazolamide. J Mol Struct. 2019;1184:225-32. doi: 10.1016/j.molstruc.2019.01.090.
37. Han J, Li L, Su M, Heng W, Wei Y, Gao Y. Deaggregation and crystallization inhibition by small amount of polymer addition for a co-amorphous curcumin-magnolol system. Pharmaceutics. 2021;13(10):1725. doi: 10.3390/pharmaceutics13101725, PMID 34684018.
38. Karagianni A, Kachrimanis K, Nikolakakis I. Co-amorphous solid dispersions for solubility and absorption improvement of drugs: composition, preparation, characterization and formulations for oral delivery. Pharmaceutics. 2018;10(3):98. doi: 10.3390/pharmaceutics10030098, PMID 30029516.
39. Ainurofiq A, Mauludin R, Mudhakir D, Soewandhi SN. A novel desloratadine-benzoic acid co-amorphous solid: preparation, characterization, and stability evaluation. Pharmaceutics. 2018;10(3):85. doi: 10.3390/pharmaceutics10030085, PMID 29986403.
40. Ding F, Cao W, Wang R, Wang N, Li A, Wei Y. Mechanistic study on transformation of coamorphous baicalein-nicotinamide to its cocrystal form. J Pharm Sci. 2023 Feb 1;112(2):513-24. doi: 10.1016/j.xphs.2022.08.031, PMID 36150469.
41. Agrawal A, Dudhedia M, Deng W, Shepard K, Zhong L, Povilaitis E. Development of tablet formulation of amorphous solid dispersions prepared by hot melt extrusion using quality by design approach. AAPS PharmSciTech. 2016;17(1):214-32. doi: 10.1208/s12249-015-0472-0, PMID 26757898.
42. Matsunaga H, Eguchi T, Nishijima K, Enomoto T, Sasaoki K, Nakamura N. Solid-state characterization of candesartan cilexetil (TCV-116): crystal structure and molecular mobility. Chem Pharm Bull. 1999;47(2):182-6. doi: 10.1248/CPB.47.182.
43. De Mello Costa AR, Marquiafavel FS, De Oliveira Lima Leite Vaz MM, Rocha BA, Pires Bueno PC, Amaral PL. Quercetin-PVP K25 solid dispersions: preparation, thermal characterization and antioxidant activity. J Therm Anal Calorim. 2011;104(1):273-8. doi: 10.1007/s10973-010-1083-3.
44. Löbmann K, Laitinen R, Grohganz H, Gordon KC, Strachan C, Rades T. Coamorphous drug systems: enhanced physical stability and dissolution rate of indomethacin and naproxen. Mol Pharm. 2011;8(5):1919-28. doi: 10.1021/mp2002973, PMID 21815614.
45. Alsalhi MS, Royall PG, Chan KL. Mechanistic study of the solubilization effect of basic amino acids on a poorly water-soluble drug. RSC Adv. 2022;12(30):19040-53. doi: 10.1039/d2ra02870k, PMID 35865577.